Magnetically Levitated Micro-Objects in the Quantum Regime

Lucas Clemente

July 26, 2010

Ludwig-Maximilians-Universität München

Faculty of Physics

Bachelor Thesis

Magnetically Levitated Micro-Objects in the Quantum Regime

Author:
Lucas Clemente

Supervisors:
Prof. Dr. Ignacio Cirac
Prof. Dr. Jan von Delft

July 26, 2010

Max-Planck-Institute of Quantum Optics

Hiermit bestätige ich, dass ich die vorliegende Arbeit selbstständig und nur unter Verwendung der angegebenen Hilfsmittel und Quellen erstellt habe.

München, July 26, 2010

Lucas Clemente

Abstract

One of the most striking phenomena in quantum mechanics is the concept of superposition. The implications of an object being in an overlap of two states are tremendous. Although superposition states have been studied in great detail for decades, very little is known about the frontier between the classical and the quantum mechanical world.

Recently a novel field became focus of research. *Quantum Optomechanics*, the manipulation of the center-of-mass motion of mechanical objects near the ground state, allows for samples of increasing size to be placed into the quantum regime. The transition of quantum mechanics and classical physics can be explored that way.

The key ingredient and limiting factor for quantum mechanical experiments is isolation. After a brief description of an idealized optomechanical setup we will therefore show a proposal [1, 2] to levitate nano-spheres inside a cavity using optical tweezers. To further enhance isolation we will then discuss the idea to use magnetic levitation on superconducting objects. This allows us to eliminate heating due to the tweezers and thus considerably extend the quantum regime to even larger objects. With the arising possibility to measure the object's position we also consider applications in feedback-cooling.

Contents

1. Introduction to Quantum Optomechanics **1**
- 1.1. Historical Development . . . 1
- 1.2. The Optomechanical Setup . . . 1
- 1.3. Classical Treatment . . . 2
- 1.4. Quantum Mechanical Treatment . . . 4

2. Laser Levitated Optomechanics **10**
- 2.1. Light-Sphere Interaction Hamiltonian . . . 11
- 2.2. Optical Trapping . . . 12
- 2.3. Optomechanical Coupling . . . 13
- 2.4. Sources of Decoherence . . . 14
  - 2.4.1. Scattering of Air Molecules . . . 14
  - 2.4.2. Scattering of Photons . . . 15

3. Magnetic Trapping **17**
- 3.1. Ferromagnetic Trapping . . . 17
- 3.2. Trapping of Superconductors . . . 18
- 3.3. Position Measurement and Feedback Cooling . . . 18

4. Outlook **20**

Appendices **21**

A. Lemmata **21**
- A.1. Unitary transformations on the Hamiltonian . . . 21
- A.2. Nonexistence of local field maxima . . . 21

B. Coherent states **23**

C. Magnetic Trap Setup **26**

D. Superposition State Generation **27**

Bibliography **29**

1. Introduction to Quantum Optomechanics

1.1. Historical Development

The field of quantum optomechanics was pioneered by James Clerk Maxwell almost 140 years ago. He proposed an effect he called *radiation pressure*, a light-induced force on matter. A simple explanation can be given in the particle picture of light, where photons colliding into an object cause a force due to their impulse. An equation for the force is easily deductible, $F = \frac{P}{c}$. As the speed of light is large compared to beam power P, the resulting force is small; it is however visible under certain circumstances (e.g. tails of comets point away from the sun as already observed by Keppler). From the 1970s the concept of radiation pressure has been used for the manipulation of small objects. Particularly with monochromatic light from lasers it is nowadays possible to trap atoms in harmonic potentials and cool them to very low temperatures.

Very recently there have been proposals taking this manipulation to the next level. With carefully engineered setups it is possible to conduct experiments near the ground state of center-of-mass motion of harmonic oscillators. Experiments with massive objects in the ground state allow totally new insights on quantum mechanics, e.g. concerning the frontier between classical and quantum physics. This field of optical manipulation of mechanical quantum states is called *Quantum Optomechanics* [3].

1.2. The Optomechanical Setup

Most quantum optomechanical experiments consist of an optical cavity, a setup where two mirrors in a certain distance face each other (similar to a Fabry-Pérot interferometer). Light coupled into the cavity is reflected multiple times between the mirrors and forms special modes inside the cavity. When the mirrors of a cavity are designed so that attenuation is very small, the system becomes very sensitive to small changes. For example tiny fluctuations in the cavity length have a massive effect on the cavity mode. This property makes cavities an interesting object of study for a wide range of experiments. As an exemplary setup[1] of a quantum optomechanical experiment we will now consider a cavity of length L. One mirror can move in a harmonic potential as shown in Fig. 1.1. The cavity is driven by a laser with frequency ω_L, its resonance frequency is called ω_c.

[1] Although we consider an idealized setup, similar experiments have been conducted with mirrors on cantilevers.

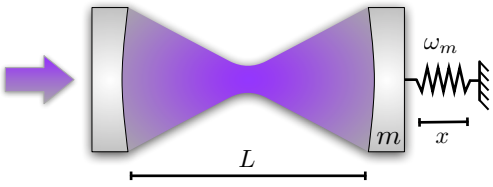

Figure 1.1.: A concentric cavity. One mirror of mass m is moving in a harmonic potential with angular frequency ω_m. The equilibrium cavity length is called L, the displacement of the mirror is x.

In this setup light reflected from the free mirror causes a radiation pressure force. This force leads to a displacement of the mirror. However, as the length of the cavity changes, the mode inside collapses, radiation pressure vanishes. The mirror in turn moves back and the cycle starts from the beginning. Obviously a stimulated oscillation emerges in this system [4, 5]. As an interesting feature radiation pressure follows the displacement with a small delay. This lag originates from the time that photons inside the cavity need to leak out (or be brought in, respectively), thus reducing (increasing) radiation pressure. The time lag is approximately the ring-down time of the cavity κ^{-1}. When the setup is precisely engineered the lag can lead to a cooling (or amplification) of the mirror movement [3, 6].

1.3. Classical Treatment

To describe the evolution of the system we will first apply a classical approach. Let x be the displacement of the moving mirror with $x = 0$ its equilibrium position without cavity field. We can then write the equation of motion of the mirror as a damped harmonic oscillator

$$m\ddot{x} = -m\omega_m^2 x - m\gamma\dot{x} + F(t) \tag{1.1}$$

where γ is the intrinsic damping rate of the spring and $F(t)$ donates the time dependent radiation pressure force. We will model this force to anneal its proper value $\mathcal{F}(x)$ exponentially with rate τ^{-1}:

$$\dot{F}(t) = \frac{\mathcal{F}(x(t)) - F(t)}{\tau} \tag{1.2}$$

As the displacement will usually be small, we can approximate $\mathcal{F}(x)$ linearly around the the equilibrium position in presence of the cavity field $\bar{x}$. Equation (1.2) then gives:

$$\dot{F}(t) = \frac{\mathcal{F}(\bar{x}) + \mathcal{F}'(\bar{x})x(t) - F(t)}{\tau} \tag{1.3}$$

Let us now go to the Fourier space. We get

$$-\omega^2 m\tilde{x}(\omega) = -m\omega_m^2\tilde{x}(\omega) - \mathrm{i}\omega m\gamma\tilde{x}(\omega) + \tilde{F}(\omega) \tag{1.4}$$

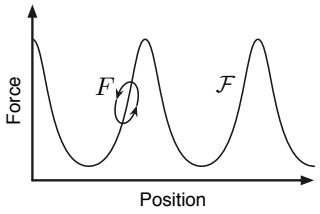

Figure 1.2.: Radiation pressure force vs. position of the mirror [9, p. 299]. If the oscillation of the mirror is engineered carefully so that it moves up and down the resonance slope, the force has a small time lag (the time that photons need to leak out of the cavity). This time lag leads to a dampening of the mirror movement.

and

$$\mathrm{i}\omega\tau\tilde{F}(\omega) = \mathcal{F}'(\bar{x})\tilde{x}(\omega) - \tilde{F}(\omega) \tag{1.5}$$

which holds for $\omega \neq 0$ as we dropped $\mathcal{F}(\bar{x})\delta(\omega)$, the Fourier transform of $\mathcal{F}(\bar{x})$. Together this gives the full equation of motion in the Fourier space

$$-\omega^2 m\tilde{x}(\omega) = -m\omega_m^2\tilde{x}(\omega) - \mathrm{i}\omega m\gamma\tilde{x}(\omega) + \frac{\mathcal{F}'(\bar{x})\tilde{x}(\omega)}{1 - \mathrm{i}\omega\tau} \tag{1.6}$$

By comparison of the intrinsic damping and the imaginary part of the last term we get the optomechanical damping rate for the frequency ω_m

$$\Gamma_{\mathrm{opt}} = \frac{1}{m\omega_m}\frac{\mathcal{F}'(\bar{x})\omega_m\tau}{1 + (\omega_m\tau)^2} \tag{1.7}$$

The derived value for optomechanical damping is not quantitatively correct. It is based on a very simple ansatz (1.1) that does not include any quantum effects (or e.g. effects from the cavity drive). However it is able to explain several important properties of the setup. As can be seen from the formula, optomechanical damping Γ_{opt} can appear if $\bar{x}$ is chosen so that $\mathcal{F}'(\bar{x}) > 0$. This corresponds to a precise placement of the oscillator on the resonance slope[1] as shown in Fig. 1.2. If the setup is engineered accordingly very low temperatures can be realized [7, 8].

[1] After entering the cavity from the left a beam of light will propagate to the right mirror and result in an electric field E_0 there. The ray will then be reflected with coefficient r from the right and the the left mirror and arrive again with field $E_0 r^2 e^{\mathrm{i}\delta}$ where $\delta = 4L\pi\lambda^{-1}$ is the phase difference. Repeating this procedure for all reflections, we obtain

$$E = E_0 \sum r^{2n} e^{\mathrm{i}\delta n}$$

As $|r^2 e^{\mathrm{i}\delta}| < 1$, we can apply the formula for a geometric series $E = E_0(1 - r^2 e^{\mathrm{i}\delta})^{-1}$. Radiation pressure is proportional to intensity [9, p. 299]

$$I \propto |E|^2 = \left|E_0(1 - r^2 e^{\mathrm{i}\delta})^{-1}\right|^2 \propto (1 + r^4 - 2r^2\cos\delta)^{-1}$$

A qualitative plot of the Lorentzian-like dependence of radiation pressure of the mirror displacement is shown in Fig. 1.2. The distance between the resonances is $\lambda/2$.

1.4. Quantum Mechanical Treatment

We previously derived the dynamics of the optomechanical setup in a classical approximation. However, as the mirror movement approaches the quantum mechanical ground state this classical description becomes inadequate. To understand the system from a quantum mechanical point of view, we first derive the Hamiltonian of the system, following [10]. From the Hamiltonian we will want to infer the mean excitation number of phonons in the mechanical oscillator.

We start by summing relevant terms for the total Hamiltonian:

$$\hat{H}_{\text{tot}} = \hat{H}_{\text{cavity}} + \hat{H}_m + \hat{H}_{\text{output}} + \hat{H}_{\text{cavity-output}} \tag{1.8}$$

where $\hat{H}_{\text{cavity}} = \omega_c(\hat{x})\hat{a}^\dagger\hat{a}$ is the cavity Hamiltonian, with $\hat{a}^\dagger\hat{a}$ the number of cavity photons, and $\hat{H}_m = \omega_m\hat{b}^\dagger\hat{b}$ is the Hamiltonian of the mechanical oscillator, with $\hat{b}^\dagger\hat{b}$ the number of phonons. As usually we have set $\hbar = 1$. Note that the cavity resonance frequency $\omega_c = \omega_c(\hat{x})$ depends on the position of the mechanical oscillator (i.e. the moving mirror). For small $\hat{x}$ we can approximate $\hat{H}_{\text{cavity}}$ linearly (cf. [11]):

$$\hat{H}_{\text{cavity}} = \omega_c(\hat{x})\hat{a}^\dagger\hat{a} \approx \omega_c(0)\hat{a}^\dagger\hat{a} + \omega_c'(0)\hat{a}^\dagger\hat{a}\hat{x} \equiv \omega_c\hat{a}^\dagger\hat{a} + g_0\hat{a}^\dagger\hat{a}(\hat{b} + \hat{b}^\dagger) \tag{1.9}$$

where we have used $\hat{x} = x_0(\hat{b}+\hat{b}^\dagger)$ and $g_0 \equiv \omega_c'(0)x_0$. Note that the correct Hamiltonian of an oscillator including the vacuum state is $\hat{H} = \omega(\hat{a}^\dagger\hat{a}+\frac{1}{2})$, however the $\frac{1}{2}$ term usually only adds a constant phase which is discarded. Here we cannot drop the term $\frac{g_0}{2}(\hat{b}+\hat{b}^\dagger)$ by this argument as it depends on the position $\hat{x}$. However this term only corresponds to a small shift of the mirror equilibrium position, which does not have implications on the system and can therefore be neglected without consequences.

The Hamiltonian of the field outside the cavity is obtained by integrating the photon number over all possible frequencies $\hat{H}_{\text{output}} = \int_0^\infty \omega\hat{a}_0^\dagger(\omega)\hat{a}_0(\omega)\mathrm{d}\omega$ where we have defined $\hat{a}_0$ as the annihilation operator of a photon outside the cavity.

The last term, the coupling of cavity and the output modes, is given by

$$\hat{H}_{\text{cavity-output}} = \mathrm{i}\int_0^\infty \gamma(\omega)(\hat{a}^\dagger\hat{a}_0(\omega) - \hat{a}_0^\dagger(\omega)\hat{a})\mathrm{d}\omega \tag{1.10}$$

This can be understood as the transition of a drive photon into the cavity ($\hat{a}^\dagger\hat{a}_0(\omega)$) and the decay of a cavity photon ($\hat{a}_0^\dagger(\omega)\hat{a}$), weighted over their rates $\gamma(\omega)$.

We now have the total Hamiltonian as

$$\hat{H}_{\text{tot}} = \omega_m\hat{b}^\dagger\hat{b} + \omega_c\hat{a}^\dagger\hat{a} + g_0\hat{a}^\dagger\hat{a}(\hat{b} + \hat{b}^\dagger) + \mathrm{i}\int_0^\infty \gamma(\omega)(\hat{a}^\dagger\hat{a}_0(\omega) - \hat{a}_0^\dagger(\omega)\hat{a})\mathrm{d}\omega + \int_0^\infty \omega\hat{a}_0^\dagger(\omega)\hat{a}_0(\omega)\mathrm{d}\omega \tag{1.11}$$

In the following we will apply several transformations on our way to the Hamiltonian in the interaction picture. First, we will move to a rotating frame. After that a displace-

ment of the operators is made to simplify the Hamiltonian. The resulting equations can then be interpreted physically.

We start by moving the cavity and the output field to a frame rotating with the laser frequency ω_L. The corresponding unitary is

$$U(t) = \exp\left[-\mathrm{i}\omega_L\left(\hat{a}^\dagger\hat{a} + \int_0^\infty \hat{a}_0^\dagger(\omega)\hat{a}_0(\omega)\mathrm{d}\omega\right)t\right] \tag{1.12}$$

Unitarity and the fact that this unitary has the desired effect can easily be shown. Note that

$$\dot{U} = -\mathrm{i}\omega_L U\left(\hat{a}^\dagger\hat{a} + \int_0^\infty \hat{a}_0^\dagger(\omega)\hat{a}_0(\omega)\mathrm{d}\omega\right) \tag{1.13}$$

The effect of the transformation on the Hamiltonian is given by $\tilde{H} = U\hat{H}U^\dagger - \mathrm{i}\dot{U}U^\dagger$ (see appendix section A.1), adopted to our unitary we get, after extracting U from $\dot{U}$:

$$\tilde{H} = U\left[\hat{H} - \omega_L\left(\hat{a}^\dagger\hat{a} + \int_0^\infty \hat{a}_0^\dagger(\omega)\hat{a}_0(\omega)\mathrm{d}\omega\right)\right]U^\dagger \tag{1.14}$$

Let us first consider the term in the squared brackets. Inserting the Hamiltonian (1.11) we get

$$\omega_m\hat{b}^\dagger\hat{b} + \Delta\hat{a}^\dagger\hat{a} + g_0\hat{a}^\dagger\hat{a}(\hat{b}+\hat{b}^\dagger) + \mathrm{i}\int_0^\infty \gamma(\omega)(\hat{a}^\dagger\hat{a}_0(\omega) - \hat{a}_0^\dagger(\omega)\hat{a})\mathrm{d}\omega + \int_0^\infty (\omega-\omega_L)\hat{a}_0^\dagger(\omega)\hat{a}_0(\omega)\mathrm{d}\omega \tag{1.15}$$

where we have introduced laser detuning $\Delta \equiv \omega_c(0) - \omega_L$. We still have to apply the unitary transformation which gives us the Hamiltonian in the rotating frame

$$\tilde{H} = \omega_m\hat{b}^\dagger\hat{b} + \Delta\hat{a}^\dagger\hat{a} + g_0\hat{a}^\dagger\hat{a}(\hat{b}+\hat{b}^\dagger) + \mathrm{i}\int_{-\omega_L}^\infty \gamma(\omega)(\hat{a}^\dagger\hat{a}_0(\omega) - \hat{a}_0^\dagger(\omega)\hat{a})\mathrm{d}\omega + \int_{-\omega_L}^\infty \omega\hat{a}_0^\dagger(\omega)\hat{a}_0(\omega)\mathrm{d}\omega \tag{1.16}$$

where we redefined $\hat{a}_0(\omega) \equiv \hat{a}_0(\omega+\omega_L)$ and $\gamma(\omega) \equiv \gamma(\omega+\omega_L)$.

In the following we will switch to a representation where we extract the coherent part of the states. This allows us to work in the Fock basis, on top of a coherent representation. Coherent states are explained in detail in the appendix in chapter B.

Let us apply the unitary displacement $\hat{D}$ of the cavity field, the mechanical field and the output mode, defined by

$$\begin{aligned}\hat{D}^\dagger\hat{a}\hat{D} &= \hat{a} + \alpha \\ \hat{D}^\dagger\hat{b}\hat{D} &= \hat{b} + \beta \\ \hat{D}^\dagger\hat{a}_0(\omega)\hat{D} &= \hat{a}_0(\omega) + \alpha_\omega(\omega)\end{aligned} \tag{1.17}$$

where we introduced

$$\alpha_\omega(\omega) = \begin{cases} \frac{\Omega}{\gamma(0)}\delta(\omega) & \text{if } \omega = 0 \\ \alpha_\omega & \text{else} \end{cases} \tag{1.18}$$

Note that for $\hat{a}_0(0)$ (which corresponds to the laser frequency in our rotating frame) we apply a different transformation. We have introduced $\Omega = 2\sqrt{P\kappa/\omega_L}$ where P is the drive laser power and κ is again the decay rate of cavity photons.

With these transformations we get the Hamiltonian

$$\begin{aligned} \hat{H}'_{\text{tot}} = {} & \omega_m \hat{b}^\dagger\hat{b} + \omega_m\beta^*\hat{b} + \omega_m\beta\hat{b}^\dagger + \omega_m|\beta|^2 \\ & + \Delta\hat{a}^\dagger\hat{a} + \Delta\alpha^*\hat{a} + \Delta\alpha\hat{a}^\dagger + \Delta|\alpha|^2 \\ & + g_0\hat{a}^\dagger\hat{a}(\hat{b}+\hat{b}^\dagger) + g_0\alpha\hat{a}^\dagger(\hat{b}+\hat{b}^\dagger) + g_0\alpha^*\hat{a}(\hat{b}+\hat{b}^\dagger) + g_0|\alpha|^2(\hat{b}+\hat{b}^\dagger) \\ & + g_0\hat{a}^\dagger\hat{a}(\beta+\beta^*) + g_0\alpha\hat{a}^\dagger(\beta+\beta^*) + g_0\alpha^*\hat{a}(\beta+\beta^*) + g_0|\alpha|^2(\beta+\beta^*) \\ & + \mathrm{i}\int_{-\omega_L}^{\infty} \gamma(\omega)(\hat{a}^\dagger\hat{a}_0(\omega) + \alpha^*\hat{a}_0(\omega) + \alpha_\omega(\omega)\hat{a}^\dagger + \alpha_\omega(\omega)\alpha^* - \text{H.c.})\mathrm{d}\omega \\ & + \int_{-\omega_L}^{\infty} \omega(\hat{a}_0^\dagger(\omega)\hat{a}_0(\omega) + \alpha_\omega^*(\omega)\hat{a}_0(\omega) + \alpha_\omega(\omega)\hat{a}_0^\dagger(\omega) + |\alpha_\omega(\omega)|^2)\mathrm{d}\omega \end{aligned} \tag{1.19}$$

Any constant shift in the Hamiltonian has no physical implication, we will therefore drop any terms not dependent of $\hat{a}$, $\hat{b}$ or $\hat{a}_0(\omega)$ or their conjugates. We define $⨍\,\mathrm{d}\omega$ as the integral over ω excluding the point $\omega = 0$. The Hamiltonian then becomes

$$\begin{aligned} \hat{H}'_{\text{tot}} = {} & \omega_m \hat{b}^\dagger\hat{b} + \omega_m\beta^*\hat{b} + \omega_m\beta\hat{b}^\dagger + \Delta\hat{a}^\dagger\hat{a} + \Delta\alpha^*\hat{a} + \Delta\alpha\hat{a}^\dagger \\ & + g_0\hat{a}^\dagger\hat{a}(\hat{b}+\hat{b}^\dagger) + g_0\alpha\hat{a}^\dagger(\hat{b}+\hat{b}^\dagger) + g_0\alpha^*\hat{a}(\hat{b}+\hat{b}^\dagger) + g_0|\alpha|^2(\hat{b}+\hat{b}^\dagger) \\ & + g_0\hat{a}^\dagger\hat{a}(\beta+\beta^*) + g_0\alpha\hat{a}^\dagger(\beta+\beta^*) + g_0\alpha^*\hat{a}(\beta+\beta^*) \\ & + \mathrm{i}\int_{-\omega_L}^{\infty} \gamma(\omega)(\hat{a}^\dagger\hat{a}_0(\omega) + \alpha^*\hat{a}_0(\omega) - \text{H.c.})\mathrm{d}\omega \\ & + \mathrm{i}⨍_{-\omega_L}^{\infty} \gamma(\omega)(\alpha_\omega\hat{a}^\dagger - \alpha_\omega^*\hat{a})\mathrm{d}\omega + \mathrm{i}\Omega\hat{a}^\dagger - \mathrm{i}\Omega\hat{a} \\ & + \int_{-\omega_L}^{\infty} \omega\hat{a}_0^\dagger(\omega)\hat{a}_0(\omega)\mathrm{d}\omega + ⨍_{-\omega_L}^{\infty} \omega(\alpha_\omega^*\hat{a}_0(\omega) + \alpha_\omega\hat{a}_0^\dagger(\omega))\mathrm{d}\omega \end{aligned} \tag{1.20}$$

Let us now choose α, β and α_ω so that terms in the Hamiltonian that have exactly one annihilation or creation operator sum up to zero. This obviously corresponds to

$$\Delta\alpha + g_0\alpha(\beta+\beta^*) + \mathrm{i}⨍_{-\omega_L}^{\infty} \gamma(\omega)\alpha_\omega\mathrm{d}\omega + \mathrm{i}\Omega = 0 \quad \text{for } \hat{a}^\dagger \tag{1.21}$$

$$\omega_m\beta + g_0|\alpha|^2 = 0 \quad \text{for } \hat{b}^\dagger \tag{1.22}$$

$$\omega\alpha_\omega - \mathrm{i}\gamma(\omega)\alpha = 0 \quad \text{for } \hat{a}_0^\dagger \tag{1.23}$$

Note that we dropped the integrals in the last line.

The solution of equations (1.22) and (1.23) can simply be written as

$$\beta = -\frac{g_0|\alpha|^2}{\omega_m} \tag{1.24}$$

and

$$\alpha_\omega = \frac{\mathrm{i}\gamma(\omega)\alpha}{\omega} \quad \text{for } \omega \neq 0 \tag{1.25}$$

As the optomechanical coupling g_0 is small compared to the other terms in (1.21) we can drop the term $g_0\alpha(\beta+\beta^*)$ in our considerations. The solution for α then becomes

$$\alpha = \frac{\Omega}{\mathrm{i}\Delta - \mathrm{i}\fint_{-\omega_L}^{\infty}\frac{\gamma^2(\omega)}{\omega}\mathrm{d}\omega} = \frac{\Omega}{\mathrm{i}\Delta + \kappa} \tag{1.26}$$

We have used that $\gamma^2(\omega) \approx \kappa/\pi$ for a finite region around $\omega = 0$:

$$\fint_{-\omega_L}^{\infty}\frac{\gamma^2(\omega)}{\omega}\mathrm{d}\omega = \frac{\kappa}{\pi}\fint_{-\omega_L}^{\infty}\frac{\mathrm{d}\omega}{\omega} = \frac{\kappa}{\pi}\lim_{\varepsilon\to 0}\int_{-\zeta}^{\zeta}\frac{\mathrm{d}\omega}{\omega+\varepsilon} = \frac{\kappa}{\pi}\lim_{\varepsilon\to 0}\log\left(\frac{\zeta+\varepsilon}{-\zeta+\varepsilon}\right) = \mathrm{i}\kappa \tag{1.27}$$

for $\omega_L > \zeta > \varepsilon$.

Let us now write the Hamiltonian without the linear terms:

$$\begin{aligned}\hat{H}'_{\mathrm{tot}} = {} & \omega_m\hat{b}^\dagger\hat{b} + \Delta\hat{a}^\dagger\hat{a} \\ & + g_0\hat{a}^\dagger\hat{a}(\hat{b}+\hat{b}^\dagger) + g_0\alpha\hat{a}^\dagger(\hat{b}+\hat{b}^\dagger) + g_0\alpha^*\hat{a}(\hat{b}+\hat{b}^\dagger) + g_0\hat{a}^\dagger\hat{a}(\beta+\beta^*) \\ & + \mathrm{i}\int_{-\omega_L}^{\infty}\gamma(\omega)(\hat{a}^\dagger\hat{a}_0(\omega) - \mathrm{H.c.})\mathrm{d}\omega + \int_{-\omega_L}^{\infty}\omega\hat{a}_0^\dagger(\omega)\hat{a}_0(\omega)\mathrm{d}\omega\end{aligned} \tag{1.28}$$

writing $\alpha = |\alpha|\mathrm{e}^{\mathrm{i}\varphi}$ and $\alpha^* = |\alpha|\mathrm{e}^{-\mathrm{i}\varphi}$ respectively we get

$$\begin{aligned}\hat{H}'_{\mathrm{tot}} = {} & \omega_m\hat{b}^\dagger\hat{b} + \Delta\hat{a}^\dagger\hat{a} \\ & + g_0|\alpha|\mathrm{e}^{\mathrm{i}\varphi}\hat{a}^\dagger(\hat{b}+\hat{b}^\dagger) + g_0|\alpha|\mathrm{e}^{-\mathrm{i}\varphi}\hat{a}(\hat{b}+\hat{b}^\dagger) \\ & + \mathrm{i}\int_{-\omega_L}^{\infty}\gamma(\omega)(\hat{a}^\dagger\hat{a}_0(\omega) - \mathrm{H.c.})\mathrm{d}\omega + \int_{-\omega_L}^{\infty}\omega\hat{a}_0^\dagger(\omega)\hat{a}_0(\omega)\mathrm{d}\omega\end{aligned} \tag{1.29}$$

Note that we dropped the terms $g_0\hat{a}^\dagger\hat{a}(\hat{b}+\hat{b}^\dagger)$ and $g_0\hat{a}^\dagger\hat{a}(\beta+\beta^*)$, as their contribution is small compared to the terms with α.

We now define $g \equiv g_0|\alpha|$ and redefine $\hat{a} \equiv \mathrm{e}^{-\mathrm{i}\varphi}\hat{a}$ which gives us the full transformed Hamiltonian:

$$\begin{aligned}\hat{H}'_{\mathrm{tot}} = {} & \omega_m\hat{b}^\dagger\hat{b} + \Delta\hat{a}^\dagger\hat{a} + g(\hat{a}+\hat{a}^\dagger)(\hat{b}+\hat{b}^\dagger) \\ & + \mathrm{i}\int_{-\omega_L}^{\infty}\gamma(\omega)(\hat{a}^\dagger\hat{a}_0(\omega)\mathrm{e}^{-\mathrm{i}\varphi} - \mathrm{H.c.})\mathrm{d}\omega + \int_{-\omega_L}^{\infty}\omega\hat{a}_0^\dagger(\omega)\hat{a}_0(\omega)\mathrm{d}\omega\end{aligned} \tag{1.30}$$

Note that as g_0 has been replaced by $g_0|\alpha| = g_0\sqrt{n_{\mathrm{photons}}}$ (see appendix B), i.e. the coupling is enhanced by the square-root of the number of photons inside the cavity. This allows us to achieve the strong coupling regime ($g > \kappa$) where the optomechanical

coupling exceeds dissipation. Strong coupling between a mechanical oscillator and the cavity field has been shown experimentally in [12].

As a last step we transform this Hamiltonian to the interaction picture. Let us therefore write it as $\hat{H}'_{\text{tot}} = \hat{H}_0 + \hat{H}_1$ where

$$\hat{H}_0 = \omega_m \hat{b}^\dagger \hat{b} + \Delta \hat{a}^\dagger \hat{a} + \int_{-\omega_L}^{\infty} \omega \hat{a}_0^\dagger(\omega)\hat{a}_0(\omega)\mathrm{d}\omega \tag{1.31}$$

and

$$\hat{H}_1 = g(\hat{a} + \hat{a}^\dagger)(\hat{b} + \hat{b}^\dagger) + \mathrm{i}\int_{-\omega_L}^{\infty} \gamma(\omega)(\hat{a}^\dagger \hat{a}_0(\omega)\mathrm{e}^{-\mathrm{i}\varphi} - \text{H.c.})\mathrm{d}\omega \tag{1.32}$$

The interesting part of the Hamiltonian in the interaction picture is

$$\hat{H}^I_{\text{tot}} = \mathrm{e}^{\mathrm{i}\hat{H}_0 t}\hat{H}_1 \mathrm{e}^{-\mathrm{i}\hat{H}_0 t} \tag{1.33}$$

This immediately gives the transformed total Hamiltonian in the interaction picture

$$\hat{H}^I_{\text{tot}} = g(\hat{a}\mathrm{e}^{-\mathrm{i}\Delta t} + \hat{a}^\dagger \mathrm{e}^{\mathrm{i}\Delta t})(\hat{b}\mathrm{e}^{-\mathrm{i}\omega_m t} + \hat{b}^\dagger \mathrm{e}^{\mathrm{i}\omega_m t}) + \mathrm{i}\int_{-\omega_L}^{\infty} \gamma(\omega)(\hat{a}^\dagger \hat{a}_0(\omega)\mathrm{e}^{\mathrm{i}\Delta t - \omega t - \varphi} - \text{H.c.})\mathrm{d}\omega \tag{1.34}$$

Let us now expand the coupling for two concrete values of laser detuning:

$$\Delta = -\omega_m \quad \Rightarrow \quad g\left[\hat{a}\hat{b} + \hat{a}\hat{b}^\dagger \mathrm{e}^{\mathrm{i}2\omega_m t} + \hat{a}^\dagger \hat{b}\mathrm{e}^{-\mathrm{i}2\omega_m t} + \hat{a}^\dagger \hat{b}\right] \tag{1.35}$$

$$\Delta = \omega_m \quad \Rightarrow \quad g\left[\hat{a}\hat{b}\mathrm{e}^{-\mathrm{i}2\omega_m t} + \hat{a}\hat{b}^\dagger + \hat{a}^\dagger \hat{b} + \hat{a}^\dagger \hat{b}\mathrm{e}^{\mathrm{i}2\omega_m t}\right] \tag{1.36}$$

The terms containing $\mathrm{e}^{\pm\mathrm{i}2\omega_m t}$ rotate very fast. On the timescale of interest they average to zero, we will therefore neglect those terms. This approximation is called *Rotating-Wave-Approximation* and is valid for $\omega_m \gg g$. We obtain two Hamiltonians:

$$\hat{H}^I_{\Delta=-\omega_m} = g(\hat{a}\hat{b} + \hat{a}^\dagger \hat{b}^\dagger) + \mathrm{i}\int_{-\omega_L}^{\infty} \gamma(\omega)(\hat{a}^\dagger \hat{a}_0(\omega)\mathrm{e}^{\mathrm{i}\Delta t - \omega t - \varphi} - \text{H.c.})\mathrm{d}\omega \tag{1.37}$$

$$\hat{H}^I_{\Delta=\omega_m} = g(\hat{a}\hat{b}^\dagger + \hat{a}^\dagger \hat{b}) + \mathrm{i}\int_{-\omega_L}^{\infty} \gamma(\omega)(\hat{a}^\dagger \hat{a}_0(\omega)\mathrm{e}^{\mathrm{i}\Delta t - \omega t - \varphi} - \text{H.c.})\mathrm{d}\omega \tag{1.38}$$

Hamiltonian (1.37) corresponds to a two-mode squeezed state interaction. We are however interested in the latter. This beam-splitter interaction corresponds to two processes:

- The annihilation of a cavity photon and a creation of a phonon on the mechanical oscillator ($\hat{a}\hat{b}^\dagger$).
- The extraction of a phonon from the mechanical oscillator and the creation of a cavity photon ($\hat{a}^\dagger \hat{b}$).

In terms of states we can write these processes as

$$|m\rangle_p|n\rangle \to |m+1\rangle_p|n-1\rangle \quad \text{and} \quad |m+1\rangle_p|n-1\rangle \to |m\rangle_p|n\rangle \tag{1.39}$$

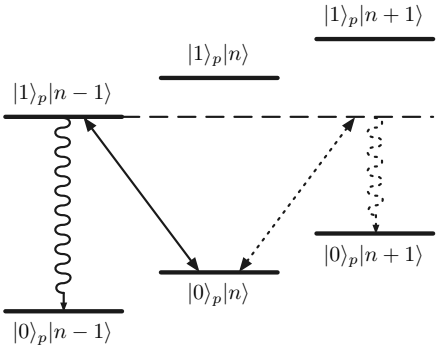

Figure 1.3.: Level diagram of the system. A phonon on the mechanical oscillator is converted into a cavity photon and back (continous line). Through dissipative effects, the cavity photon may decay before it is absorbed by the oscillator, leading to a cooling of the system state. The sqeezing process (dashed line) is prohibited by energy requirement. $|0\rangle_c$, $|1\rangle_c$ (instead of $|m\rangle_c$, $|m+1\rangle_c$) denote the Fock states of the cavity in the shifted representation.

where $|m\rangle_p$ is the photonic cavity state with m photons and $|n\rangle$ is the mechanical oscillator state with n phonons. Obviously these two processes form a cycle (cf. Fig. 1.3). However, when the system is in the excited state $|m+1\rangle_p|n-1\rangle$ dissipation can lead to a drop of the cavity state to $|m\rangle_p|n-1\rangle$ where the cycle starts again. Over time this dissipation leads to a cooling of the mechanical state, similar to sideband cooling used with ions. Note that other possible processes are prohibited by energy requirements as posed by the laser drive.

From the Hamiltonian (1.38) we can derive an interesting quantity, the mean number of phonons on the mechanical oscillator through optomechanical considerations $\bar{n}_m^0$. We skip long calculations (see [13, 14] or [15]) and directly give the resulting formula

$$\bar{n}_m^0 = \left(\frac{\kappa}{4\omega_m}\right)^2 \tag{1.40}$$

This result however only includes effects due to our idealized setup. In reality we will we have further couplings to consider (e.g. Brownian motion), we obtain

$$\bar{n}_m = \left(\frac{\kappa}{4\omega_m}\right)^2 + \frac{\Gamma+}{\Gamma_-} \tag{1.41}$$

where the $\Gamma_\pm$ donate the heating and cooling rates of other effects that contribute to the resulting phonon number. Equation (1.41) shows that ground state cooling $\bar{n}_m < 1$ can be achieved in the resolved sideband regime $\omega_m \gg \kappa$ and $\Gamma_- \gg \Gamma_+$.

We have derived the Hamiltonian of the typical optomechanical setup, seen that passive cooling is possible through dissipation and given the mean excitation number of the mechanical oscillator. Let us now look into physical implementations.

2. Laser Levitated Optomechanics

After the theoretical description of the idealized quantum optomechanical experiment in the previous section we will now focus on a physical implementation as proposed in [1, 2]. Let us however first recall crucial requirements to the setup: The cavity should be of good quality, i.e. photon decay rate κ is small. Additionally, mechanical trapping ω_m has to be strong and mechanical dissipation γ_m small. The latter is particularly obvious, as mechanical dissipation is equal to thermal contact, resulting in a heating of the oscillator state. In several setups with cantilevers, microscopic mirrors (see e.g. [4, 16]) which are all connected physically to the environment, this coupling has been a major source of decoherence.

In our setup we will minimize coupling to the environment by levitating the mechanical oscillator, a dielectric sphere in the sub-micrometer range, in the free vacuum. This is achieved by trapping the mechanical oscillator in a harmonic potential using optical tweezers. The setup is shown in Fig. 2.1. In the following we will focus on the coupling of the dielectric sphere to the laser field. We start by deriving the interaction Hamiltonian, then show that trapping with optical tweezers is possible. After that we will derive the optomechanical coupling and analyze sources of decoherence in this setup. A protocol for the subsequent creation of a superposition state $|\psi\rangle = \frac{1}{\sqrt{2}}(|0\rangle \pm |1\rangle)$ from the displaced ground state is described in appendix D. Our discussion follows [10].

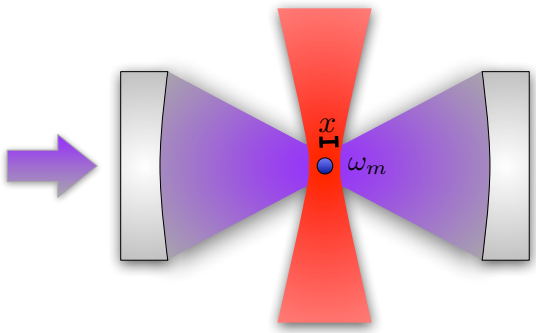

Figure 2.1.: The setup from [1]. A dielectric nano-sphere is trapped by optical tweezers (red) inside a cavity. Its center of mass motion operates as mechanical oscillator and can be cooled to the ground state similar to the moving mirror. Note that both mirrors are fixed in this setup.

2.1. Light-Sphere Interaction Hamiltonian

Let us start our discussion of this setup by deriving a Hamiltonian to describe the macroscopic interaction of the dielectric sphere and light. The Hamiltonian for an ensemble of atoms in an electric field is given by

$$\hat{H}_{\mathrm{LM}} = \hat{H}_{\mathrm{A}} + \hat{H}_{\mathrm{rad}} + \hat{H}_{\mathrm{int}} \tag{2.1}$$

$$= \sum_i \frac{1}{2}\nu_0\sigma_{z,i} + \int \mathrm{d}^3k\omega_{\mathbf{k}}\hat{a}^\dagger(\mathbf{k})\hat{a}(\mathbf{k}) - \sum_i d_i E_i \tag{2.2}$$

The first term is the atomic energy of a two-level system with energy difference ν_0 between ground and excited state, $\sigma_{z,i}$ is the Pauli matrix. The second term is the energy of a free electric field, where $\hat{a}^\dagger(\mathbf{k})$ is the creation operator of a photon with frequency $\omega_{\mathbf{k}}$ and wave vector $\mathbf{k}$. The last term is the interaction of the atomic dipole moment $d_i = \mathcal{P}(\sigma_{+,i} + \sigma_{-,i})$ and the electric field

$$E_i = E(\mathbf{x_i}) = \frac{\mathrm{i}}{(2\pi)^{3/2}} \int \mathrm{d}^3k \sqrt{\frac{\omega_{\mathbf{k}}}{2\varepsilon_0}} (\mathrm{e}^{-\mathrm{i}\mathbf{k}\mathbf{x_i}}\hat{a}(\mathbf{k}) - \mathrm{H.c.}) \tag{2.3}$$

When we go to the continuous limit we replace the transition operators $\sigma_{\pm,i}$ by $\sigma_\pm(\mathbf{x}) \equiv \lim_{V\to 0} \sigma_{\pm,i}/V$. To prevent double-counting of the particle-particle interactions we add the factor $\frac{1}{2}$ to the interaction term:

$$\hat{H}_{\mathrm{LM}} = \int \mathrm{d}^3x \frac{1}{2}\nu_0\sigma_z(\mathbf{x}) + \int \mathrm{d}^3k\omega_{\mathbf{k}}\hat{a}^\dagger(\mathbf{k})\hat{a}(\mathbf{k}) - \frac{1}{2}\int \mathrm{d}^3x\mathcal{P}(\sigma_+(\mathbf{x}) + \sigma_-(\mathbf{x}))E(\mathbf{x}) \tag{2.4}$$

Let us now derive the equation of motion of the $\sigma_\pm$. Using Heisenberg's equation we get

$$\frac{\mathrm{d}}{\mathrm{d}t}\sigma_+(\mathbf{x}) = -\mathrm{i}[\sigma_+(\mathbf{x}), \hat{H}_{\mathrm{LM}}] \tag{2.5}$$

$$= -\mathrm{i}\frac{1}{2}\nu_0[\sigma_+(\mathbf{x}), \sigma_z(\mathbf{x})] + \frac{\mathrm{i}\mathcal{P}}{2}E(\mathbf{x})[\sigma_+(\mathbf{x}), \sigma_+(\mathbf{x}) + \sigma_-(\mathbf{x})] \tag{2.6}$$

$$= \mathrm{i}\nu_0\sigma_+(\mathbf{x}) - \mathrm{i}\frac{2\mathcal{P}}{V}E(\mathbf{x}) \tag{2.7}$$

where we assumed all atoms to be in the ground state $\sigma_z = -1/V$ where V is the volume of the sphere.

Next we transform σ_+ to the rotating frame $\tilde{\sigma}_+(\mathbf{x}) = \mathrm{e}^{\mathrm{i}\omega_L t}\sigma_+(\mathbf{x})$. When writing $E(\mathbf{x}) = \tilde{E}^{(+)}(\mathbf{x})\mathrm{e}^{-\mathrm{i}\omega_L t} + \tilde{E}^{(-)}(\mathbf{x})\mathrm{e}^{\mathrm{i}\omega_L t}$ the equation of motion (2.7) becomes

$$\frac{\mathrm{d}}{\mathrm{d}t}\tilde{\sigma}_+(\mathbf{x}) = \mathrm{i}\omega_L\tilde{\sigma}_+(\mathbf{x}) + \mathrm{e}^{\mathrm{i}\omega_L t}\frac{\mathrm{d}}{\mathrm{d}t}\sigma_+(\mathbf{x}) \tag{2.8}$$

$$= \mathrm{i}(\omega_L - \nu_0)\tilde{\sigma}_+(\mathbf{x}) - \frac{\mathrm{i}2\mathcal{P}}{V}(\tilde{E}^{(+)}(\mathbf{x})\mathrm{e}^{-\mathrm{i}\omega_L t} + \tilde{E}^{(-)}(\mathbf{x})\mathrm{e}^{\mathrm{i}\omega_L t})\mathrm{e}^{\mathrm{i}\omega_L t} \tag{2.9}$$

Performing a rotating wave approximation we get

$$\frac{\mathrm{d}}{\mathrm{d}t}\tilde{\sigma}_{\pm}(\mathbf{x}) \approx \mathrm{i}\Delta\tilde{\sigma}_{+}(\mathbf{x}) - \frac{\mathrm{i}2\mathcal{P}}{V}\tilde{E}^{(\pm)}(\mathbf{x}) \tag{2.10}$$

where $\Delta = \omega_L - \nu_0$.

We now perform an adiabatic elimination, i.e. we set the slowly-varying terms to zero, $\mathrm{d}\tilde{\sigma}_{\pm}(\mathbf{x})/\mathrm{d}t \approx 0$. When we drop the same phases we get

$$\sigma_{\pm}(\mathbf{x}) = \frac{2\mathcal{P}}{V\Delta}E^{(\pm)}(\mathbf{x}) \tag{2.11}$$

With that we can write the polarization as

$$P = \mathcal{P}(\sigma_{+}(\mathbf{x}) + \sigma_{-}(\mathbf{x})) = \frac{2\mathcal{P}^2}{V\Delta}E(\mathbf{x}) \tag{2.12}$$

Let us compare this result to the macroscopic equation for the polarization (i.e. the Clausius-Mosotti-Relation)

$$\text{Macroscopic:} \quad P = 3\varepsilon_0\frac{\varepsilon_r - 1}{\varepsilon_r + 2}E \tag{2.13}$$

$$\text{Microscopic:} \quad P = \frac{2\mathcal{P}^2}{V\Delta}E \tag{2.14}$$

Obviously we have

$$\frac{2\mathcal{P}^2}{V\Delta} = 3\varepsilon_0\frac{\varepsilon_r - 1}{\varepsilon_r + 2} \tag{2.15}$$

We can therefore write the interaction part of Hamiltonian (2.4) as

$$\hat{H}_{\mathrm{int}} = -\frac{\varepsilon_c}{2}\int_{V(\mathbf{r})}\mathrm{d}^3x|E(\mathbf{x})|^2 \tag{2.16}$$

where we defined $\varepsilon_c \equiv 3\varepsilon_0(\varepsilon_r - 1)/(\varepsilon_r + 2)$ and again, we have assumed all atoms to be in the ground state so that the term $\int \mathrm{d}^3x\frac{1}{2}\nu_0\sigma_z(\mathbf{x})$ only adds a constant energy shift. Note that the integral has to be evaluated over the volume of the object $V(\mathbf{r})$, depending on its center-of-mass position $\mathbf{r}$.

2.2. Optical Trapping

We will now apply the derived sphere-field interaction Hamiltonian to show that trapping a sphere with optical tweezers is possible [17–21]. We assume a Gaussian beam in direction y (cf. Fig. 2.1)

$$|E(y,r)| = E_0\frac{W_0}{W(y)}\exp\left(-\frac{r^2}{W(y)^2}\right) \tag{2.17}$$

Here W_0 is the beam waist and $W(y) = W_0\sqrt{1+(y\lambda/(\pi W_0^2))^2}$ its width. Developing $|E(x,y,z)|^2$ in second order around $y = r = 0$ we get

$$|E(y,r)|^2 \approx E_0^2 - \frac{E_0^2 y^2 \lambda^2}{\pi^2 W_0^2} + r^2\left(-\frac{2E_0^2}{W_0^2} + \frac{4E_0^2 y^2\lambda^2}{\pi^2 W_0^4}\right) \tag{2.18}$$

We insert this into Hamiltonian (2.16) and drop constant terms:

$$\hat{H}_{\mathrm{LM}} = -\frac{\varepsilon_c}{2}\int_{V(\mathbf{r})} \mathrm{d}^3x |E(\mathbf{x})|^2 \tag{2.19}$$

$$\approx -\frac{\varepsilon_c}{2} V |E(\mathbf{x})|^2 \tag{2.20}$$

$$= -\frac{\varepsilon_c}{2} V E_0^2 \left[r^2\left(\frac{4y^2\lambda^2}{\pi^2 W_0^4} - \frac{2}{W_0^2}\right) - \frac{y^2\lambda^2}{\pi^2 W_0^2}\right] \tag{2.21}$$

As y is very small compared to waist size, we get the harmonic trapping

$$\hat{H}_{\mathrm{LM}} \approx \varepsilon_c V E_0^2 r^2 \frac{1}{W_0^2} \equiv \frac{1}{2} M\omega_m^2 r^2 \tag{2.22}$$

Replacing $E_0^2 \approx 2I/(c\varepsilon_0)$ where I is the beam intensity and inserting ε_c we obtain the trapping frequency perpendicular to y:

$$\omega_m^2 = \frac{12I}{\varrho c \varepsilon_0 W_0^2}\left(\frac{\varepsilon_r - 1}{\varepsilon_r + 2}\right) \tag{2.23}$$

Typically this trapping frequency is of the order of several MHz.

2.3. Optomechanical Coupling

We have shown that optical tweezers are able to trap a dielectric object harmonically. In the following we will focus in the coupling between the sphere and the cavity field. Coupling to the output-field as a source of decoherence will be discussed in section 2.4.

Recall the coupling Hamiltonian (1.9)

$$\hat{H} = \int d^3k \omega_{\mathbf{k}} \hat{a}^\dagger \hat{a} + g_0 \hat{a}^\dagger \hat{a}(\hat{b} + \hat{b}^\dagger) \tag{2.24}$$

We will now calculate the coupling strength g_0 for the proposed setup. We assume the sphere to be placed at a knot (i.e. a point of maximum slope) of the standing wave inside the cavity. For small displacements we can approximate the TEM_{00} mode cavity field by

$$|E(\mathbf{r})|^2 \approx \frac{\omega_c}{\varepsilon_0 \pi W_0^2 L}\left(1 - \frac{2r^2}{W_0^2}\right)\cos^2\left(\frac{\omega_c x}{c}\right)\hat{a}^\dagger\hat{a} \tag{2.25}$$

Again, $W_0 = \sqrt{\lambda L/(2\pi)}$ is the field's waist size, λ is the laser wavelength and L is the cavity length. Plugging this into the light matter Hamiltonian (2.16) we get

$$\hat{H}_{\text{coupling}} = -\omega_c \hat{a}^\dagger \hat{a} \frac{3V(\varepsilon_r - 1)[W_0^2 - 2r^2]\cos^2\left(\frac{\omega_c x}{c} - \frac{\pi}{4}\right)}{(\varepsilon_r + 2)\pi W_0^4 L} \tag{2.26}$$

where the phase shift of $\pi/4$ comes from placing the sphere at a knot. Setting $z = 0$ and developing in first order around $x = 0$ we get

$$\hat{H}_{\text{coupling}} \approx -\hat{a}^\dagger \hat{a} \frac{3V(\varepsilon_r - 1)\omega_c^2 \hat{x}}{(\varepsilon_r + 2)c\pi W_0^2 L} \tag{2.27}$$

During the development $\cos^2(x + \pi/4) \approx 1/2 + x$ we dropped the term $1/2$. This term does not contribute to the coupling, however it gives the contribution of the sphere to the resonance frequency of the cavity.

Let us now quantize $\hat{x} = x_0(\hat{b} + \hat{b}^\dagger)$, we get

$$\hat{H}_{\text{coupling}} = -\hat{a}^\dagger \hat{a}(\hat{b} + \hat{b}^\dagger) x_0 \frac{3V(\varepsilon_r - 1)\omega_c}{(\varepsilon_r + 2)c\pi W_0^2 L} \tag{2.28}$$

By comparing this to (1.9) we get

$$g_0 = -x_0 \frac{3\omega_c(\varepsilon_r - 1)V}{(\varepsilon_r + 2)cL\pi W_0^2} \tag{2.29}$$

When we plug in numbers into this equation we get a coupling of $g_0 \approx 10\text{Hz}$, which is much smaller than κ. Recall however, that the effective coupling $g = g_0|\alpha| = g_0\sqrt{n_{\text{photon}}}$ is much larger, as the number of photons in the cavity is of the order of 10^{10}. We get an optomechanical coupling in the MHz range within the regime $g > \kappa$.

2.4. Sources of Decoherence

2.4.1. Scattering of Air Molecules

In this section we will derive the heating rate due to collisions with air particles [1, 22]. We assume the air molecules to be of mass m and mean velocity $\bar{v}$. The pressure inside the vacuum chamber is P, the temperature is T, the density is ϱ. We start with the equation of motion for the sphere

$$\ddot{x} + 2\gamma\dot{x} + \omega_m^2 x = \xi(t) \tag{2.30}$$

Here $\xi(t)$ is the stochastic force of the air molecules. We assume white noise $\langle \xi(t)\xi(t')\rangle = 2M^2 D\delta(t - t')$ where we have introduced the diffusion constant $D = 2k_B T\gamma/M$. We will first derive a value for γ from kinetic gas theory.

Let v be the sphere's velocity. We move to the reference frame in that the sphere is stationary. In this frame, a third (one dimension) of the particles is relevant, those

collide into the sphere with velocity $\bar{v} - v$ from behind and with velocity $\bar{v} + v$ from the front. We get the change of momentum as

$$\frac{\mathrm{d}p}{\mathrm{d}t} = (\bar{v} - v)^2 \pi R^2 \frac{\varrho}{3m} 2m - (\bar{v} + v)^2 \pi R^2 \frac{\varrho}{3m} 2m \tag{2.31}$$

$$= -\frac{4\pi R^2 \varrho \bar{v}}{3M} 2Mv \equiv -\gamma 2Mv \tag{2.32}$$

With $\varrho = 3P/\bar{v}^2$ we get

$$\gamma = \frac{4\pi R^2 P}{M\bar{v}} \tag{2.33}$$

Solving the stochastic differential equation (2.30) requires some calculations which we omit here. We can derive the variance of the position

$$\mathrm{Var}(x) = \langle x^2(t) \rangle \approx \frac{D}{2\gamma\omega_m^2}(1 - \mathrm{e}^{-2\gamma t}) \tag{2.34}$$

Using the equipartition theorem we can compute the increase of energy in time as $\Delta E(t) = M\omega_m^2 \,\mathrm{Var}(x)$. We define the time t^* as $\Delta E(t^*) = \omega_m$, i.e. as the time that is needed for one quantum of energy to be absorbed by the mechanical oscillator. We get

$$t^* = -\frac{1}{2\gamma} \log\left(1 - \frac{\omega_m}{k_B T}\right) \approx \frac{\omega_m}{k_B T 2\gamma} \tag{2.35}$$

As $\Gamma_{\mathrm{air}} = 1/t^*$ we have

$$\Gamma_{\mathrm{air}} = \frac{2\gamma k_B T}{\omega_m} = \frac{8\pi R^2 P k_B T}{M\omega_m \sqrt{3k_B T/m}} \tag{2.36}$$

where we replaced $\bar{v} = \sqrt{3k_B T/m}$ with $m \approx 28.6\mathrm{u}$.

With this equation we get feasible values at room temperature of approximately $P \approx 10^{-6}\mathrm{torr}$ and $\gamma \approx 1\mathrm{mHz}$. The quality factor $Q = \omega_m/\gamma$ is of the order of 10^9.

2.4.2. Scattering of Photons

Besides the noise from air molecules we also have to consider decoherence due to the lasers. Both, tweezer and cavity photons are scattered on the sphere. However, as the sphere is very small, the scattering events corresponds to a stochastical process. We can analyze this with a Markovian approach. Without derivation we give the heating rates:

$$\Gamma_{\mathrm{tweezers}} = 3\frac{P}{\omega_L \pi W_0^2} \left(\frac{\varepsilon_r - 1}{\varepsilon_r + 2}\right)^2 V \frac{k_c^6 c}{2\pi\varrho\omega_m} \tag{2.37}$$

and

$$\Gamma_{\text{cavity}} = 3|\alpha|^2 \left(\frac{\varepsilon_r - 1}{\varepsilon_r + 2}\right)^2 V \frac{k_c^6 c}{2\pi V_c \varrho \omega_m} \cos^2 \frac{\omega_c x}{c} \tag{2.38}$$

where k_c is the wave vector of the photons, P is the tweezers' intensity and $V_c = \pi W_0^2 L$ is the cavity volume.

Additionally to the scattering of photons, the perturbation of the cavity field also leads to a decrease of the cavity's quality, i.e. the photon decay rate κ is increased. This limits the sphere size to several hundred nanometers for a typical cavity setup.

3. Magnetic Trapping

As shown in section 2.4 the primary sources of decoherence of our setup are Brownian motion of air molecules in the vacuum, scattering of cavity photons and heating from the tweezers. Especially the latter two drastically limit the size of the object. In the following we will discuss possibilities to replace the tweezers by magnetic alternatives. We will consider ferromagnetic trapping first in section 3.1, superconducting objects in section 3.2. As the results of those sections are not limited to the described setup we will consider the possibility to measure the object's position inductively and use this information for feedback cooling in section 3.3.

3.1. Ferromagnetic Trapping

Magnetic trapping of neutral particles has been a field of research for several years. Proposals for the trapping of neutral atoms have been made [23–25] and experimentally achieved [17, 19, 26, 27]. We will first lay out the basics of trapping neutral atoms and small objects with magnetic traps.

The potential energy of a particle with permanent magnetic moment $\vec{\mu}$ in a magnetic field with strength $\vec{B}$ is $U = -\vec{\mu} \cdot \vec{B}$. For elementary particles (like the neutron) there exist only two possible directions of spin and therefore only two possible directions of the magnetic moment relative to B. In the parallel alignment the particles tend to go into the direction of higher fields whereas they are repelled in the antiparallel case. Particles that are drawn to high fields are called *high-field seeker*, particles that go towards minima are called *low-field seeker*. As it is not possible to create a local maximum of a static magnetic field (see appendix A.2 for a proof) only low-field seekers may be trapped in a static magnetic field. However, low-field seeking particles are subject to spin-flip processes as their energy in the field is higher than that of high-field seeker. In addition, macroscopic objects do not show quantization of their magnetic moment and are therefore high-field seeking.

We have seen that it is impossible to trap neutral object with static fields. An idea would be to use dynamic fields rotating in a way that their average over time forms a local maximum. As shown in [24] this is possible, however the particle's motion inside a dynamic trap consists of two parts: a slow guiding center motion and a very fast oscillating part. Unless the latter can be prohibited in some way, ferromagnetic trapping with dynamic fields is no alternative. Another downside of dynamic fields oscillating with frequencies well over 10^6Hz is that they induce high currents in other parts of the setup, disturbing measurements and creating noise.

3.2. Trapping of Superconductors

Let us now evaluate the possibility to trap a diamagnet in a static magnetic field. Free diamagnets in a static magnetic field behave as low-field seekers. Their magnetization is linear with the external magnetic field $M = \chi H$, however the magnetic susceptibility is $\chi < 0$. As $M = \mu/V$ and $H = B/\mu_0$ we have the potential

$$U = -\mu B = -MVB = -\chi HVB = -\frac{\chi V}{\mu_0} B^2 \tag{3.1}$$

Assuming a linear magnetic field $B(x) = \alpha x$ we get the harmonic potential

$$U = -\frac{\chi V \alpha^2}{\mu_0} x^2 \equiv \frac{m\omega_m^2}{2} x^2 \tag{3.2}$$

By replacing $m/V \equiv \varrho$ we obtain the trap frequency

$$\omega_m = \alpha \sqrt{2 \frac{|\chi|}{\mu_0 \varrho}} \tag{3.3}$$

If we insert values of typical diamagnets, $\chi \approx -10^{-5}$ and $\varrho \approx 1\mathrm{g/cm^3}$ we get the estimation $\omega[\mathrm{Hz}] \approx 0.1 \cdot \alpha[T/m]$. We would need gradients of about 10^7T/m (10^9G/cm) which will not be feasible for static magnetic fields in the near future. However, using a superconductor ($\chi = -1$) gives a huge advantage. We get as an estimation $\omega[\mathrm{Hz}] \approx 40 \cdot \alpha[T/m]$, which gives $\omega = 10^6$Hz for $\alpha \approx 25$T/mm or $\alpha = 2.5 \cdot 10^6$G/cm. This is in the upper bound of the feasible range for experimental implementation [28, 29]. A possible method for the generation of field minima with high gradients is sketched in appendix C.

Using a superconductor brings along some other implications. Most importantly it has to be cooled first and should not be heated over the critical temperature during the experiment. However both requirements are not difficult to fulfill, as mechanical coupling is reduced to a minimum anyway and the magnetic trap will be cooled to a superconducting state itself. Especially for high-temperature superconductors like $HgBa_2Ca_2Cu_3O_x$ with a critical temperature of $T_C = 133$K [30] cooling should be feasible.

3.3. Position Measurement and Feedback Cooling

An important feature of superconductors is that they behave as perfect diamagnets ($\chi = -1$). This allowed us to increase the trapping frequency by several orders of magnitude compared to other diamagnets as discussed in section 3.2. A perfect diamagnet expels any magnetic field from its inside; the field in the superconductor is approximately zero[1] (cf. Fig. 3.1). Obviously this leads to a higher field in the vicinity of the superconducting sphere. We assume that the magnetic field outside of the superconductor decays as $1/x^3$,

[1] The magnetic field inside a superconductor decays with $1/r^2$ as given by the London-Equation.

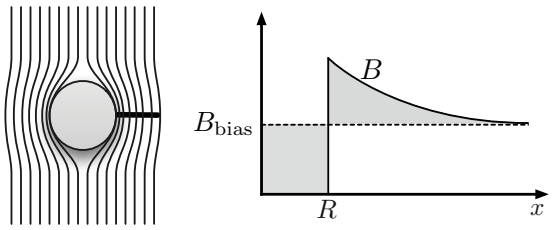

Figure 3.1.: Left: Magnetic field lines are expelled from the superconductor. Right: The estimation used for the magnetic field. After radius R the decay $1/x^3$ is chosen so that the two gray areas are of the same size. The dashed line represents the field in the absence of an object.

normalized so that the following condition is fulfilled (cf. Fig. 3.1):

$$RB_{\text{bias}} = \int_R^\infty (B(x) - B_{\text{bias}})\mathrm{d}x \tag{3.4}$$

This approximation is based on the idea that $\int B\mathrm{d}V$ stays the same with or without an object in the field, justified by $\nabla \cdot \mathbf{B} = 0$.

With $B(x) = B_{\text{bias}} + a/x^3$ we get

$$B(x) = B_{\text{bias}} \left(1 + 2\frac{R^3}{x^3}\right) \tag{3.5}$$

Let us now estimate the change of B at a fixed position in distance R from the sphere surface when the sphere moves by a tiny amount, the ground state size x_0. We have

$$\Delta B = B(2R) - B(2R + x_0) = 2B_{\text{bias}}R^3 \left[\frac{1}{8R^3} - \left(\frac{2\omega_m M}{\hbar}\right)^{3/2}\right] \tag{3.6}$$

For $R = 1\mu\text{m}$, $\varrho = 1\text{g/cm}^3$ and $B_{\text{bias}} = 1\text{T}$ we get $\Delta B \approx 0.1\mu\text{T}$. This lies well in the possible range for a measurement with SQUIDs [31–33], even with a strong bias field [34]. Therefore it should be possible to measure the position of the sphere inside a magnetic trap with a SQUID.

Most interestingly, information about the position of an object in a trap allows much simpler types of cooling. Feedback cooling should be applicable for the given regime. Additionally all photonic sources of decoherence are eliminated, which allows for much larger spheres. Decoherence due to the magnetic trapping and position measurement will be discussed elsewhere.

4. Outlook

We have shown the basics of backaction cooling on an exemplary setup with a cavity and a cantilever. To address the problem of thermal contact, we analyzed levitated mechanical oscillators trapped by optical tweezers. We derived the interaction of a levitated sphere, the tweezers and the cavity field and discussed sources of decoherence.

Ground state cooling in this scheme is possible, however photonic decoherence from the lasers limits the object size to several hundred nanometers. To eliminate this drawback we have analyzed the possibility to use ferromagnetic or superconducting objects, levitated by magnetic fields. Magnetic trapping of superconductors could replace lasers in future experiments, decreasing decoherence by several orders of magnitude.

In addition to magnetic levitation, we proposed a way of inductively measuring the position of the oscillator. Although a thorougher analysis of this system has to be performed, our results suggest experimental feasibility of feedback cooling for spheres larger than several microns.

Besides being of interest for quantum information theory, all proposed setups allow a unique insight into the very basics of quantum mechanics. The frontier between classical mechanics and the quantum regime can be examined; macroscopic objects can be brought into a quantum superposition state. It may even be possible to place small living organisms like viruses or other objects inside a hollow sphere and perform quantum mechanical experiments with them. Schrödinger's cat could soon prove to be more than a theoretical paradigm after all.

A. Lemmata

A.1. Unitary transformations on the Hamiltonian

In this section we will show how to write the Hamiltonian of a system transformed by a unitary U of the form $U = \exp(-\mathrm{i}A)$ with $A = A^\dagger$. We start with the density matrix of the new frame $\tilde{\varrho} = U\varrho U^\dagger$. As an effect of this transformation the Heisenberg equation $\dot{\varrho} = \mathrm{i}[\hat{H}, \varrho]$ becomes:

$$\begin{aligned}
\dot{\tilde{\varrho}} &= \dot{U}\varrho U^\dagger + U\dot{\varrho}U^\dagger + U\varrho\dot{U}^\dagger \\
&= \dot{U}U^\dagger U\varrho U^\dagger + \mathrm{i}U[H,\varrho]U^\dagger + U\varrho U^\dagger U\dot{U}^\dagger \\
&= \dot{U}U^\dagger\tilde{\varrho} + \mathrm{i}UH\varrho U^\dagger - \mathrm{i}U\varrho HU^\dagger + \tilde{\varrho}U\dot{U}^\dagger \\
&= \dot{U}U^\dagger\tilde{\varrho} + \mathrm{i}UHU^\dagger U\varrho U^\dagger - \mathrm{i}U\varrho U^\dagger UHU^\dagger - \tilde{\varrho}\dot{U}U\dagger \\
&= \dot{U}U^\dagger\tilde{\varrho} + \mathrm{i}UHU^\dagger\tilde{\varrho} - \mathrm{i}\tilde{\varrho}UHU^\dagger - \tilde{\varrho}\dot{U}U^\dagger \\
&= [\dot{U}U^\dagger + \mathrm{i}UHU^\dagger, \tilde{\varrho}] \\
&= \mathrm{i}[UHU^\dagger - \mathrm{i}\dot{U}U^\dagger, \tilde{\varrho}] \\
&\equiv \mathrm{i}[\tilde{H}, \tilde{\varrho}]
\end{aligned}$$

where we have used $U\dot{U}^\dagger = -\dot{U}U^\dagger$, which is obvious as U may be written as $U = \exp(-\mathrm{i}\tilde{U})$. We see that the transformed Hamiltonian is $\tilde{H} = UHU^\dagger - \mathrm{i}\dot{U}U^\dagger$.

A.2. Nonexistence of local field maxima

In this section we will prove a theorem on local field maxima [23, 35]. Let us state the theorem as

Theorem. *In a region without charges and currents, neither a static electric nor static magnetic field may have local maxima*[1].

Proof. Let $\mathbf{E}$ be either an electric or a magnetic field. W.l.o.g. let a local maximum $|\mathbf{E}|$ be at the origin. Then for any point $\mathbf{r}$ the electric field can be written as

$$\mathbf{E}(\mathbf{r}) = \mathbf{E}(\mathbf{0}) + \delta\mathbf{E} \tag{A.1}$$

and

$$\mathbf{E}^2(\mathbf{r}) = \mathbf{E}^2(\mathbf{0}) + 2\mathbf{E}(\mathbf{0}) \cdot \delta\mathbf{E} + (\delta\mathbf{E})^2 \tag{A.2}$$

[1] Remark: The same holds for a gravitational field.

Obviously on the right side of (A.2) the first and the last term are positive. As $\mathbf{E}(\mathbf{0})$ is a local maximum we require $\mathbf{E}(\mathbf{0})\delta\mathbf{E} < 0$ for arbitrary $\mathbf{r}$ near $\mathbf{0}$. Let us now take the $\hat{z}$ axis along $\mathbf{E}(\mathbf{0})$, we get $\mathbf{E}(\mathbf{0}) \cdot \delta\mathbf{E} = E_z(\mathbf{0})\delta E_z$. As $E_z(\mathbf{0}) > 0$ we have

$$\delta E_z(\mathbf{r}) < 0 \quad \text{for arbitrary } \mathbf{r} \text{ near } 0 \tag{A.3}$$

We will now show that this condition is in conflict with electrodynamics.

Using Gauss' theorem combined with Maxwell's law $\nabla \cdot \mathbf{E} = 0$ (in absence of charges or currents, $\rho = 0$ and $\mathbf{j} = \mathbf{0}$) on a sphere centered around $\mathbf{0}$ we get

$$\int_V \nabla\delta\mathbf{E}\mathrm{d}V = 0 = \int_{\partial V} \delta\mathbf{E} \cdot \mathrm{d}\mathbf{A} \tag{A.4}$$

We see that this is in conflict to (A.3), as $\delta E_z < 0$ somewhere necessarily leads to $\delta E_z > 0$ at another point. Clearly our assumption of a local maximum is falsified.

□

B. Coherent states

In this chapter we will give a short introduction to the concept of coherent states (cf. [36, pp. 12-15], [37]). In contrast to Fock states $|n\rangle$ which are suitable to express high energy photons where the photon number is small, coherent states are convenient to use to express e.g. laser fields. They are the quantum states nearest to classical physics, as the uncertainty between phase and photon number is minimal for coherent states.

Coherent states are usually generated by the unitary *displacement operator*

$$D(\alpha) = \exp(\alpha\hat{a}^\dagger - \alpha^*\hat{a}) \tag{B.1}$$

We can also write this operator using

$$\mathrm{e}^{A+B} = \mathrm{e}^A\mathrm{e}^B\mathrm{e}^{-[A,B]/2} \tag{B.2}$$

if $[A,[A,B]] = [B,[A,B]] = 0$. Applying this theorem to (B.1) we get

$$D(\alpha) = \mathrm{e}^{-|\alpha|^2/2}\mathrm{e}^{\alpha\hat{a}^\dagger}\mathrm{e}^{-\alpha^*\hat{a}} \tag{B.3}$$

as $-[\alpha\hat{a}^\dagger, -\alpha^*\hat{a}]/2 = |\alpha|^2/2[\hat{a}^\dagger,\hat{a}] = -|\alpha|^2/2$.

In this form several properties of the displacement operator are visible:

- $D^\dagger(\alpha) = D^{-1}(\alpha) = D(-\alpha)$ which is obvious by applying the operator theorem (as $[\alpha^*\hat{a} - \alpha\hat{a}^\dagger, \alpha\hat{a}^\dagger - \alpha^*\hat{a}] = 0$).
- $D^\dagger(\alpha)\hat{a}D(\alpha) = \hat{a} + \alpha$, similar to the translation operator on a state ket [38, pp. 44ff.].
- $D^\dagger(\alpha)\hat{a}^\dagger D(\alpha) = \hat{a}^\dagger + \alpha^*$
- $D(\alpha+\beta) = D(\alpha)D(\beta)\exp(-\mathrm{i}\Im(\alpha\beta^*))$

We now define the coherent state $|\alpha\rangle$ as the result of the displacement operator acting on the vacuum state

$$|\alpha\rangle = D(\alpha)|0\rangle \tag{B.4}$$

Coherent states are eigenstates of the annihilation operator:

$$\hat{a}|\alpha\rangle = D(\alpha)D^\dagger(\alpha)\hat{a}|\alpha\rangle = D(\alpha)D^\dagger(\alpha)\hat{a}D(\alpha)|0\rangle = D(\alpha)(\hat{a}+\alpha)|0\rangle = D(\alpha)\alpha|0\rangle = \alpha|\alpha\rangle \tag{B.5}$$

An important property of coherent states is that they contain an indefinite number of photons. To derive the distribution we expand a coherent state in the Fock state basis by multiplying the eigenvalue equation (B.5) with $\langle n|$ on both sides:

$$\alpha\langle n|\alpha\rangle = \langle n|\hat{a}|\alpha\rangle = \sqrt{n+1}\langle n+1|\alpha\rangle \tag{B.6}$$

From this recursion relation it follows that

$$\langle n|\alpha\rangle = \frac{\alpha^n}{\sqrt{n!}}\langle 0|\alpha\rangle \tag{B.7}$$

We can therefore write

$$|\alpha\rangle = \sum_n |n\rangle\langle n|\alpha\rangle = \langle 0|\alpha\rangle \sum_n \frac{\alpha^n}{\sqrt{n!}}|n\rangle \tag{B.8}$$

The length of $|\alpha\rangle$ follows as

$$|\langle\alpha|\alpha\rangle|^2 = |\langle 0|\alpha\rangle|^2 \sum_n \frac{|\alpha|^{2n}}{n!} = |\langle 0|\alpha\rangle|^2 \mathrm{e}^{|\alpha|^2} \tag{B.9}$$

Furthermore

$$\langle 0|\alpha\rangle = \langle 0|D(\alpha)|0\rangle = \mathrm{e}^{-|\alpha|^2/2}\langle 0|\mathrm{e}^{\alpha\hat{a}^\dagger}\mathrm{e}^{-\alpha^*\hat{a}}|0\rangle = \mathrm{e}^{-|\alpha|^2/2} \tag{B.10}$$

Combining (B.9) and (B.10) shows that $|\langle\alpha|\alpha\rangle|^2 = 1$, i.e. coherent states are normalized. Additionally we can write the coherent state as

$$|\alpha\rangle = \mathrm{e}^{-|\alpha|^2/2} \sum_n \frac{\alpha^n}{\sqrt{n!}}|n\rangle \tag{B.11}$$

The probability distribution of the number of photons is given by

$$P(n) = |\langle n|\alpha\rangle|^2 = \frac{|\alpha|^2\mathrm{e}^{-|\alpha|^2}}{n!} \tag{B.12}$$

Note that this is a Poisson distribution, we can deduce the mean number of photons

$$\bar{n} = \langle\alpha|\hat{a}^\dagger\hat{a}|\alpha\rangle = |\alpha|^2 \tag{B.13}$$

In the following we will prove the completeness of the set of coherent states. Consider therefor the scalar product of two coherent states

$$\langle\beta|\alpha\rangle = \langle 0|D^\dagger(\beta)D(\alpha)|0\rangle \tag{B.14}$$

Using the operator theorem (B.3) we obtain

$$\langle\beta|\alpha\rangle = \exp\left[-\frac{1}{2}(|\alpha|^2 + |\beta|^2) + \alpha\beta^*\right] \tag{B.15}$$

or

$$|\langle\beta|\alpha\rangle|^2 = \mathrm{e}^{-|\alpha-\beta|^2} \tag{B.16}$$

We see that two states $|\alpha\rangle$ and $|\beta\rangle$ are *not* orthogonal, but approach orthogonality for $|\alpha - \beta| \gg 1$. Despite that we can prove completeness[1]

$$\frac{1}{\pi}\int |\alpha\rangle\langle\alpha|\mathrm{d}^2\alpha = 1 \tag{B.17}$$

Expanding using (B.11) gives:

$$\frac{1}{\pi}\int |\alpha\rangle\langle\alpha|\mathrm{d}^2\alpha = \sum_n\sum_m \frac{|n\rangle\langle m|}{\pi\sqrt{n!m!}}\int \mathrm{e}^{-|\alpha|^2}(\alpha^*)^m\alpha^n\mathrm{d}^2\alpha \tag{B.18}$$

We change to polar coordinates $\alpha = r\mathrm{e}^{\mathrm{i}\theta}$ and separate the integrals:

$$\frac{1}{\pi}\int |\alpha\rangle\langle\alpha|\mathrm{d}^2\alpha = \sum_n\sum_m \frac{|n\rangle\langle m|}{\pi\sqrt{n!m!}}\int_0^\infty \mathrm{d}r r\mathrm{e}^{-r^2}r^{n+m}\int_0^{2\pi}\mathrm{d}\theta\mathrm{e}^{\mathrm{i}(n-m)\theta} \tag{B.19}$$

With

$$\int_0^{2\pi}\mathrm{d}\theta\mathrm{e}^{\mathrm{i}(n-m)\theta} = 2\pi\delta_{nm} \tag{B.20}$$

we get

$$\frac{1}{\pi}\int |\alpha\rangle\langle\alpha|\mathrm{d}^2\alpha = \sum_n \frac{|n\rangle\langle n|}{n!}\int_0^\infty \mathrm{d}r 2r\mathrm{e}^{-r^2}r^{2n} \tag{B.21}$$

Substituting $\varepsilon = r^2$ gives

$$\frac{1}{\pi}\int |\alpha\rangle\langle\alpha|\mathrm{d}^2\alpha = \sum_n \frac{|n\rangle\langle n|}{n!}\int_0^\infty \mathrm{d}\varepsilon\mathrm{e}^{-\varepsilon}\varepsilon^n \tag{B.22}$$

As the integral equals $n!$ we obtain from the completeness of the Fock states

$$\frac{1}{\pi}\int |\alpha\rangle\langle\alpha|\mathrm{d}^2\alpha = \sum_n |n\rangle\langle n| = 1 \tag{B.23}$$

Coherent states thus form a complete basis.

Especially in laser physics, coherent states have physical significance. For example a highly stabilized laser has a field in a coherent state, other radiation fields may often easily be represented in the basis of coherent states.

[1] Coherent states are actually over-complete, however we will not prove this here.

C. Magnetic Trap Setup

In this chapter we will outline the ideas behind a magnetic trap setup [39]. For simplicity we will restrict our discussion to two dimensions, we actually discuss a linear quadrupole waveguide. However a 3d-trap can easily be found by similar considerations. Recall from section 3.2 that we need a linear magnetic field to get a harmonic potential.

Consider an infinite, straight conducting wire with current I placed in a perpendicular bias field B_0 (see Fig. C.1). The resulting field is

$$\mathbf{B} = \begin{pmatrix} B_0 \\ 0 \end{pmatrix} + \frac{I\mu_0}{2\pi(x^2+y^2)} \begin{pmatrix} -y \\ x \end{pmatrix} \tag{C.1}$$

Note that this field vanished for

$$x = 0 \quad \text{and} \quad y = \frac{I\mu_0}{2\pi B_0} \equiv r_0 \tag{C.2}$$

In a polar coordinate system with center at this position the field is

$$|\mathbf{B}(r,\varphi)| = \frac{I\mu_0}{2\pi r_0} \frac{r}{\sqrt{r^2 + r_0^2 + 2rr_0\cos\varphi}} \tag{C.3}$$

Note that this field is linear near the trap center. The gradient of this trap is given by

$$\partial_r B|\mathbf{B}(r)| = \frac{\mu_0}{2\pi} \frac{I}{r_0^2} \tag{C.4}$$

With this setup the required gradients are difficult to achieve, however it provides an insight into trap design.

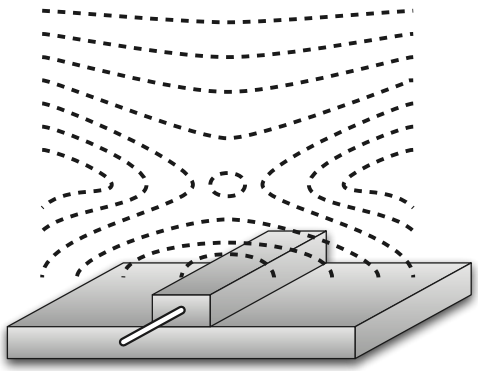

Figure C.1.: A linear quadrupole waveguide. A conducting wire is placed in a bias field which creates a minimum of the magnetic field.

D. Superposition State Generation

In the following we are going to describe a protocol from [1, 10] for the generation of superposition states, once the mechanical oscillator has been cooled to the ground state. Our goal is to create the states

$$|\psi\rangle = \frac{1}{\sqrt{2}}(|0\rangle \pm |1\rangle) \tag{D.1}$$

The protocol consists of several steps:

1. Cool the mechanical oscillator to the ground state as described previously. Leave the detuning on when the ground state is reached.
2. Send a photon of frequency ω_c into the cavity.
3. The photon will enter the cavity with probability $\frac{1}{2}$, otherwise be reflected. We therefore create a quantum state

$$|\psi\rangle = \frac{1}{\sqrt{2}}(|\text{photon inside}\rangle + |\text{photon reflected}\rangle) \tag{D.2}$$

4. The part of the photon that entered the cavity is subjected to the beam splitter interaction (1.38), $\hat{H} = g(\hat{a}\hat{b}^\dagger + \hat{a}^\dagger\hat{b})$ which leads to a time development of the state

$$|\psi\rangle_{\text{inside}}(t) = \mathrm{e}^{-\mathrm{i}\hat{H}t}|1\rangle_c|0\rangle_m \tag{D.3}$$

   where $|1\rangle_c$ denotes the state of the additional photon inside the cavity and $|0\rangle_m$ the ground state of the mechanical oscillator.

5. We wait until this interaction has exactly swapped the states, resulting in

$$|\psi\rangle_{\text{inside}}(t^*) = |0\rangle_c|1\rangle_m \tag{D.4}$$

6. Switch of the laser drive. The coupling g collapses, the mechanical oscillator photon cannot decay. We have the total state

$$|\psi\rangle = \frac{1}{\sqrt{2}}(|1\rangle_p|0\rangle_m + \mathrm{e}^{\mathrm{i}\phi}|0\rangle_p|1\rangle_m) \tag{D.5}$$

   where the first part comes from the part of the photon that did not enter the cavity and the second part with fixed phase ϕ comes from the optomechanical

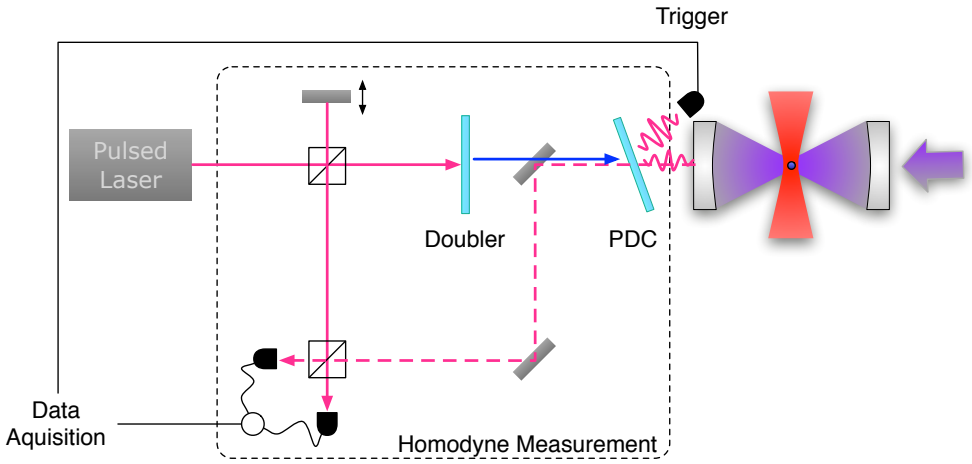

Figure D.1.: A possible setup to create the state (D.1). A photon from the pulsed laser is sent into the cavity. Part of the photon is reflected into the homodyne detector, the other part continues and couples to the mechanical oscillator state. With the measurement of the outside part the mechanical state collapses to the desired superposition.

interaction. Note that this corresponds to an entanglement of the photon outside the cavity (subscript p) and the mechanical oscillator.

7. Perform a balanced homodyne measurement of the reflected photon part in the basis $|0\rangle \pm |1\rangle$. This collapses the mechanical oscillator state to

$$|\psi\rangle_m = \frac{1}{\sqrt{2}}(|0\rangle \pm |1\rangle) \tag{D.6}$$

An experimental implementation of this protocol is shown in Fig. D.1.

The described protocol still has several flaws, especially the homodyne measurement is difficult to implement. Possible extensions in the future will work with time varying coupling parameters. The photon will be transmitted fully into the cavity and will couple to the mechanical oscillator, producing state (D.1) without any measurement.

Bibliography

[1] O. Romero-Isart, M. Juan, R. Quidant and I. Cirac – "Toward quantum superposition of living organisms", *New Journal of Physics* **12** (2010).

[2] D. E. Chang, C. A. Regal, S. B. Papp, D. J. Wilson, O. Painter, H. J. Kimble and P. Zoller – "Cavity optomechanics using an optically levitated nanosphere", *arXiv* **quant-ph** (2009).

[3] F. Marquardt and S. Girvin – "Optomechanics", *Physics* **2** (2009).

[4] T. Kippenberg and K. Vahala – "Cavity optomechanics: back-action at the mesoscale", *Science* **321** (2008).

[5] I. Favero and K. Karrai – "Optomechanics of deformable optical cavities", *Nature Photonics* **3** (2009).

[6] V. Braginsky and S. Vyatchanin – "Low quantum noise tranquilizer for fabry-perot interferometer", *Physics Letters A* **293** (2002).

[7] C. Metzger and K. Karrai – "Cavity cooling of a microlever", *Nature* **432** (2004).

[8] F. Marquardta, A. Clerkb and S. Girvinc – "Quantum theory of optomechanical cooling", *Journal of Modern Optics* **55** (2008).

[9] M. A. Nielsen and I. L. Chuang – "Quantum computation and quantum information", (2000).

[10] O. Romero-Isart, A. C. Pflanzer, M. L. Juan, R. Quidant, N. Kiesel, M. Aspelmeyer and J. I. Cirac – "Levitating nano-dieletrics in the quantum regime: theory and protocols", *manuscript in preparation.*

[11] C. K. Law – "Interaction between a moving mirror and radiation pressure: A hamiltonian formulation", *Physical Review A* **51** (1995).

[12] S. Gröblacher, K. Hammerer, M. Vanner and M. Aspelmeyer – "Observation of strong coupling between a micromechanical resonator and an optical cavity field", *Nature* **460** (2009).

[13] I. Wilson-Rae, N. Nooshi, J. Dobrindt, T. Kippenberg and W. Zwerger – "Cavity-assisted backaction cooling of mechanical resonators", *New Journal of Physics* **10** (2008).

[14] I. Wilson-Rae, N. Nooshi, W. Zwerger and T. Kippenberg – "Theory of ground state cooling of a mechanical oscillator using dynamical backaction", *Physical Review Letters* **99** (2007).

[15] F. Marquardt, J. Chen, A. Clerk and S. Girvin – "Quantum theory of cavity-assisted sideband cooling of mechanical motion", *Physical Review Letters* **99** (2007).

[16] M. Aspelmeyer, S. Groeblacher, K. Hammerer and N. Kiesel – "Quantum optomechanics - throwing a glance", *arXiv* **quant-ph** (2010).

[17] S. Chu, J. Bjorkholm, A. Ashkin and A. Cable – "Experimental observation of optically trapped atoms", *Physical Review Letters* **57** (1986).

[18] A. Ashkin, J. Dziedzic and J. Bjorkholm – "Observation of a single-beam gradient force optical trap for dielectric particles", *Optical Letters* **11** (1986).

[19] W. Paul – "Electromagnetic traps for charged and neutral particles", *Reviews of Modern Physics* **62** (1990).

[20] D. Stamper-Kurn, M. Andrews and A. Chikkatur – "Optical confinement of a bose-einstein condensate", *Physical Review Letters* **80** (1998).

[21] K. Neuman and S. Block – "Optical trapping", *Review of Scientific Instruments* **75** (2004).

[22] R. Kubo – "The fluctuation-dissipation theorem", *Reports on Progress in Physics* **29** (1966).

[23] W. Wing – "On neutral particle trapping in quasistatic electromagnetic fields", *Progress in Quantum Electronics* **8** (1984).

[24] R. Lovelace, C. Mehanian, T. Tommila and D. Lee – "Magnetic confinement of a neutral gas", *nature.com* **318** (1985).

[25] E. Peik – "Electrodynamic trap for neutral atoms", *The European Physical Journal D* **6** (1999).

[26] E. Cornell, C. Monroe and C. Wieman – "Multiply loaded, ac magnetic trap for neutral atoms", *Physical Review Letters* **67** (1991).

[27] J. Weinstein and K. Libbrecht – "Microscopic magnetic traps for neutral atoms", *Physical Review A* **52** (1995).

[28] V. Vuletic, T. Fischer, M. Praeger and T. Hänsch – "Microscopic magnetic quadrupole trap for neutral atoms with extreme adiabatic compression", *Physical Review Letters* **80** (1998).

[29] N. Chaure, F. Rhen, J. Hilton and J. Coey – "Design and application of a magnetic field gradient electrode", *Electrochemistry Communications* **9** (2007).

[30] S. Lee, S. Lee, M. Mun and M. Bae – "Synthesis and superconductivity of the hgba2ca2cu3ox superconductors", *Physica C: Superconductivity* **235-240** (1994).

[31] R. Jaklevic, J. Lambe, A. Silver and J. Mercereau – "Quantum interference effects in josephson tunneling", *Physical Review Letters* **12** (1964).

[32] M. Martínez-Pérez, J. Sesé, F. Luis and D. Drung – "Note: Highly sensitive superconducting quantum interference device microsusceptometers operating at high frequencies and very low temperatures inside the mixing chamber of a dilution refrigerator", *Review of Scientific Instruments* **81** (2010).

[33] D. Drung, C. Aßmann, J. Beyer, A. Kirste, M. Peters, F. Ruede and T. Schurig – "Highly sensitive and easy-to-use squid sensors", *IEEE Transactions on Applied Superconductivity* **17** (2007).

[34] L. Chen, W. Wernsdorfer, C. Lampropoulos, G. Christou and I. Chiorescu – "On-chip squid measurements in the presence of high magnetic fields", *arXiv* **cond-mat.mes-hall** (2010).

[35] W. Ketterle and D. Pritchard – "Trapping and focusing ground state atoms with static fields", *Applied Physics B: Lasers and Optics* **54** (1992).

[36] D. F. Walls and G. J. Milburn – "Quantum optics", (2008).

[37] R. Glauber – "Coherent and incoherent states of the radiation field", *Physical Review* **131** (1963).

[38] J. J. Sakurai and S. F. Tuan – "Modern quantum mechanics", (1994).

[39] J. Fortágh and C. Zimmermann – "Magnetic microtraps for ultracold atoms", *Reviews of Modern Physics* **79** (2007).

[40] D. Bouwmeester, A. K. Ekert and A. Zeilinger – "The physics of quantum information: quantum cryptography, quantum teleportation, quantum computation", (2000).

[41] Ö. O. Soykal and M. E. Flatté – "Strong-field interactions between a nanomagnet and a photonic cavity", *arXiv* **cond-mat.mes-hall** (2009).

[42] M. Aspelmeyer – "Quantum mechanics: The surf is up", *Nature* **464** (2010).

[43] L. Alsop, A. Goodman and F. Gustavson – "A numerical solution of a model for a superconductor field problem", *Journal of Computational Physics* **31** (1979).

[44] Ö. O. Soykal and M. E. Flatté – "Size-dependence of strong-coupling between nanomagnets and photonic cavities", *arXiv* **cond-mat.mes-hall** (2010).

[45] C. A. Dartora and G. G. Cabrera – "Quantum dynamics of molecular nanomagnets in a resonant cavity and the maser effect", *arXiv* **cond-mat.mes-hall** (2006).

[46] N. Brahms and D. M. Stamper-Kurn – "Cavity spin optodynamics", *arXiv* **quant-ph** (2010).

[47] M. Bordag and I. G. Pirozhenko – "The low temperature corrections to the casimir force between a sphere and a plane", *arXiv* **quant-ph** (2010).

[48] W. Meissner and R. Ochsenfeld – "Ein neuer effekt bei eintritt der supraleitfähigkeit", *Naturwissenschaften* **44** (1933).

[49] T. Li, S. Kheifets, D. Medellin and M. Raizen – "Measurement of the instantaneous velocity of a brownian particle", *Science* **328** (2010).

[50] V. Braginsky, S. Strigin and S. Vyatchanin – "Analysis of parametric oscillatory instability in power recycled ligo interferometer", *Physics Letters A* **305** (2002).

[51] Y. Guan, W. E. Bailey, E. Vescovo, C. C. Kao and D. A. Arena – "Time-domain measurement of driven ferromagnetic resonance", *arXiv* **cond-mat.mtrl-sci** (2006).